

Power Flow Control of STATCOM and UPFC in Distribution System

S. Saravana Kumar*, S. Sankar **, M. Padmarasan ***, C. T. Mani Kandan

****Professor, Dept of IT, Panimalar Institute of Technology, Chennai,

** Professor, Dept of EEE, Panimalar Institute of Technology, Chennai,

***Assistant Professor(G-I), Dept of EEE, Panimalar Institute of Technology, Chennai.

Abstract: This paper not only describes the closed loop reactive power control design procedure but also deals with the study on the application of the Static VAR Compensator for the control of such power in distribution system. Furthermore, the dynamic behavior of the system is analyzed in this paper the operating circuit model of VAR Compensator and Unified Power flow Controller were simulated. The simulation results agree with the theoretical results. This simulation tests under various transient conditions are analyzed this results obtained may lead to correct design of a robust controller for reactive power applications.

Index Terms: FACTS controllers, FACTS, power electronic equipment, Control, PWM

I. Introduction

Improved utilization of the existing power system is provided through the application of advanced control technologies. Power electronics based equipment, or Flexible AC Transmission Systems (FACTS), provide proven technical solutions to address these new operating challenges being presented today. FACTS technologies allow for improved transmission system operation with minimal infrastructure investment, environmental impact, and implementation time compared to the construction of new transmission lines. Traditional solutions to upgrading the electrical transmission system infrastructure have been primarily in the form of new transmission lines, substations, and associated equipment.

However, as experiences have proven over the past decade or more, the process to permit, site, and construct new transmission lines has become extremely difficult, expensive, time-consuming, and controversial. FACTS technologies provide advanced solutions as cost-effective alternatives to new transmission line construction. The potential benefits of FACTS equipment are now widely recognized by the power systems engineering and T&D communities.

With respect to FACTS equipment, voltage sourced converter (VSC) technology, which utilizes self commutated thyristors and various transistors such as GTOs, GCTs, IGCTs, and IGBTs, has been successfully applied in a number of installations world wide for static synchronous compensators [1-5], Unified Power Flow Controllers (UPFC) [6, 7], Convertible Series Compensators (CSC) [8], back-to-back dc ties (VSC-BTB) [9, 10] and VSC transmission [11].

II. Mathematical Model Of The SVC

In the Fig.1 shows a simplified equivalent circuit of the SVC [12]. Using matrix form, the mathematical model is given by

$$\frac{d}{dt} \begin{bmatrix} i_a \\ i_b \\ i_c \end{bmatrix} = \begin{bmatrix} -\frac{R}{L} & 0 & 0 \\ 0 & -\frac{R}{L} & 0 \\ 0 & 0 & -\frac{R}{L} \end{bmatrix} \begin{bmatrix} i_a \\ i_b \\ i_c \end{bmatrix} + \frac{1}{L} \begin{bmatrix} v_a - e_a \\ v_b - e_b \\ v_c - e_c \end{bmatrix} \quad (1)$$

The model of the inverter output voltage is given by

$$\begin{bmatrix} e_a \\ e_b \\ e_c \end{bmatrix} = \frac{1}{3} \begin{bmatrix} 2 & -1 & -1 \\ -1 & 2 & -1 \\ -1 & -1 & 2 \end{bmatrix} \left\{ \begin{bmatrix} S_{1A} \cdot S_{2A} \\ S_{1B} \cdot S_{2B} \\ S_{1C} \cdot S_{2C} \end{bmatrix} U_{c1} - \begin{bmatrix} S_{3A} \cdot S_{4A} \\ S_{3B} \cdot S_{4B} \\ S_{3C} \cdot S_{4C} \end{bmatrix} U_{c2} \right\} \quad (2)$$

With:

S_{ki} : The switching function, is either 1 or 0 corresponding to on and off states of the switch Q_{ki} respectively.

K : Names of arms (A, B ,C).

i : number of switches of one arm ($i = 1,2,3,4$)

The DC side currents are given by

$$\begin{aligned} I_{C1} &= S_{1A} \cdot S_{2A} \cdot i_A + S_{1B} \cdot S_{2B} \cdot i_B + S_{1C} \cdot S_{2C} \cdot i_C \\ I_{C2} &= S_{3A} \cdot S_{4A} \cdot i_A + S_{3B} \cdot S_{4B} \cdot i_B + S_{3C} \cdot S_{4C} \cdot i_C \end{aligned} \quad (3)$$

$$I_{C0} = I_{C1} + I_{C2} \quad (4)$$

And the DC side capacitor voltages are given by

$$\frac{d}{dt} \begin{bmatrix} U_{c1} \\ U_{c2} \end{bmatrix} = \frac{1}{C} \begin{bmatrix} I_{C1} \\ I_{C2} \end{bmatrix} \quad (5)$$

Equations (1) to (4) represent the mathematical model of the STATCOM in ABC Frame.

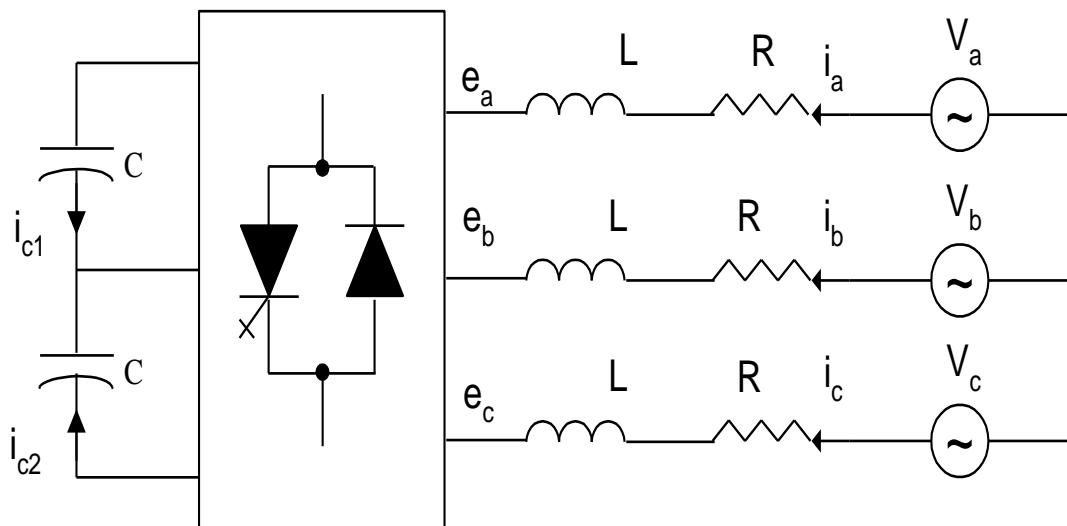


Fig.1. Equivalent Circuit of the ASVC

III. Series Compensator

Fig.2 represents the SVC connected to Network bus for regulating the local load reactive power.

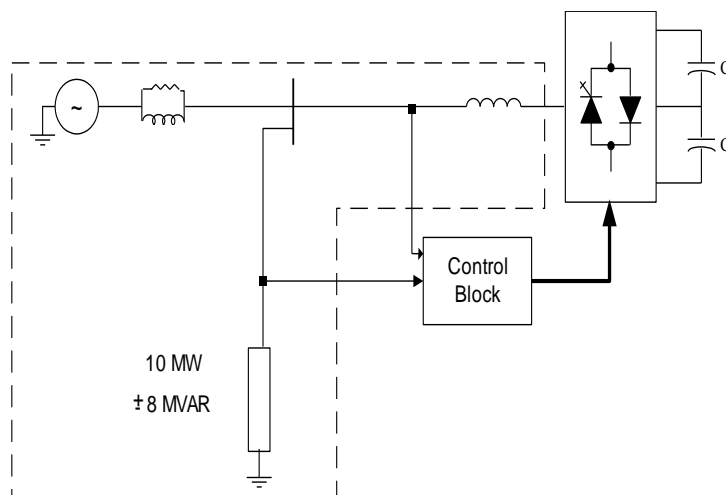


Fig.2. STATCOM connected to the network

The control of the SVC was designed to compensate the reactive power of the local load.

To achieve a simple design of the control, equations depicted above must be transformed in d-q Frame and linearized under the following assumptions [6].

- Disturbance Δ is small
- The second-order terms are dropped
- The quiescent operating point is near zero

The annotation Δ is introduced to indicate the perturbed values.

We obtain equation (6) in state space form

$$\frac{d}{dt} \begin{bmatrix} \Delta i_{qo} \\ \Delta i_{do} \\ \Delta U_{co} \end{bmatrix} = \begin{bmatrix} -R/L & -\omega & 0 \\ \omega & -R/L & -D/L \\ 0 & D/2C & 0 \end{bmatrix} \begin{bmatrix} \Delta i_{qo} \\ \Delta i_{do} \\ \Delta U_{co} \end{bmatrix} + \frac{1}{L} \begin{bmatrix} -V_L \\ 0 \\ 0 \end{bmatrix} \cdot \Delta \alpha \quad (6)$$

$$\Delta Q_c = \begin{bmatrix} -V_L & 0 & 0 \end{bmatrix} \begin{bmatrix} \Delta i_{qo} \\ \Delta i_{do} \\ \Delta U_{co} \end{bmatrix}$$

Small signal equivalent model system is used to calculate the transfer function of the system equation (7).

$$G(s) = \frac{\Delta Q_c(s)}{\Delta \alpha(s)} = \frac{A(s)}{B(s)} \quad (7)$$

$$A(s) = \frac{V_L^2}{L} \left[s^2 + \frac{R}{L}s + \frac{D^2}{2LC} \right]$$

$$B(s) = s^3 + \frac{2R}{L}s^2 + \left\{ \left[\frac{R}{L} \right]^2 + \frac{D^2}{2LC} + \omega^2 \right\} s + \frac{D^2 R}{2L^2 C}$$

IV. Transient Simulation

To check the validity of the model described above a set of simulation tests have been carried out to analyse the system under steady state and transient conditions. Based on the model of the inverter and the network described, a Simulink model depicted by Fig.3 was built.

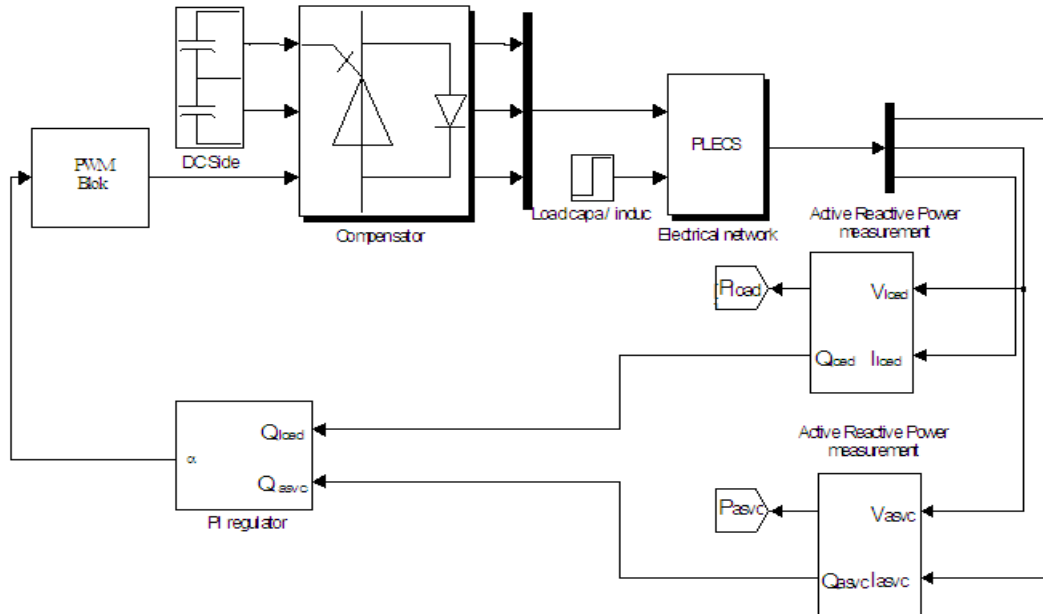


Fig.3. Simulink model of the system

Figures 4 and 5 represent the dynamic response of the compensator for switching from capacitive to inductive mode of reactive load. Figure 4 illustrates the variation of load and SVC reactive power, it shows that the compensator has a good response. At the time of 0.5 sec we connect the SVC to the line bus thus absorbing inductive power; the load is in capacitive mode. At the time of 2 sec the SVC is generating leading VARs whereas the load is in inductive mode.

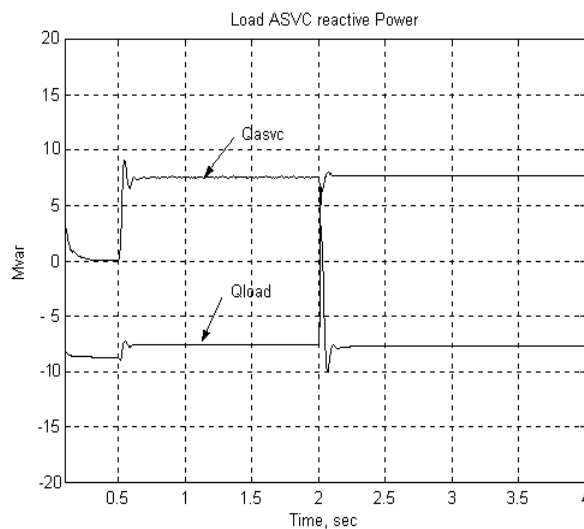


Fig.4. Reactive power variation of the load and SVC

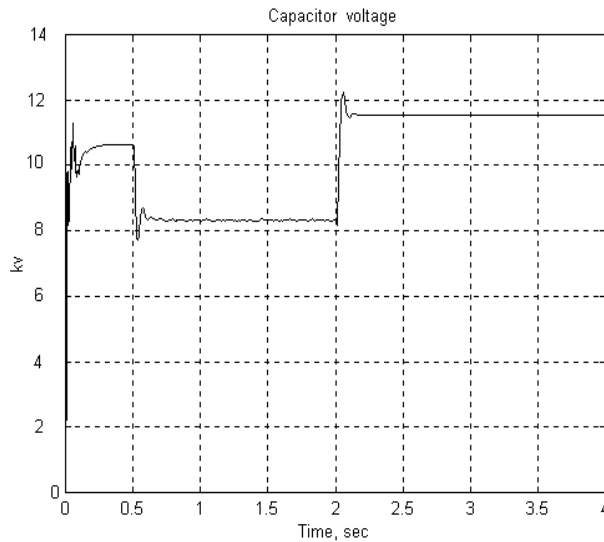


Fig.5. Dc side voltage variation

V. Unified Power Flow Controller

Consider the simple two-machine transmission model shown above. The source of variable phase angle is inserted at the midpoint of a model. Mid point is the best location because, the voltage drops along uncompensated transmission line is the largest at the midpoint. The compensation at mid point breaks the transmission line into two equal segments for each of which transmittable power is the same. By varying the phase angle of midpoint source, the real power transmitted can be varied. When the phase angle of midpoint source is set at values 60 and 270 degrees, the corresponding Variation in real power is shown in the results below. Thus by controlling the phase angle of midpoint source, the flow of real power can be controlled. The simulation circuit of UPFC is as shown in the Fig. 6.

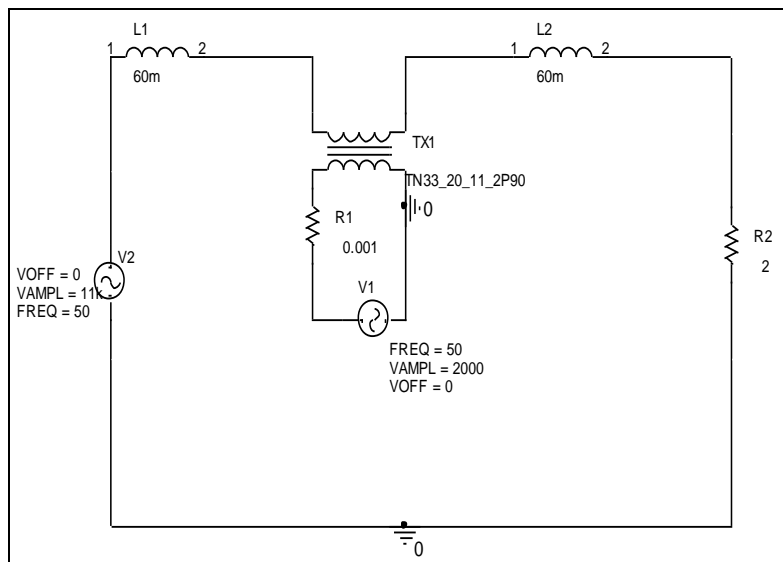


Fig .6. Simulation Circuit of UPFC

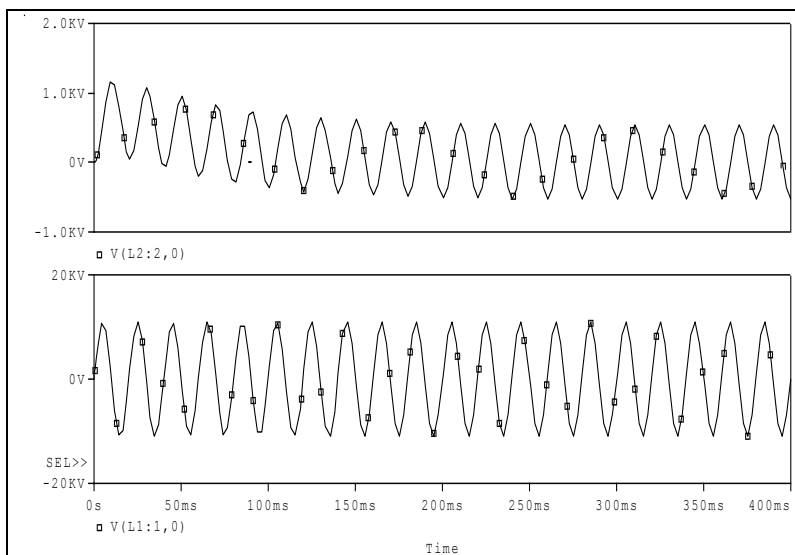


Fig. 6(a) Sending and receiving End voltages for an angle of injection at 60°

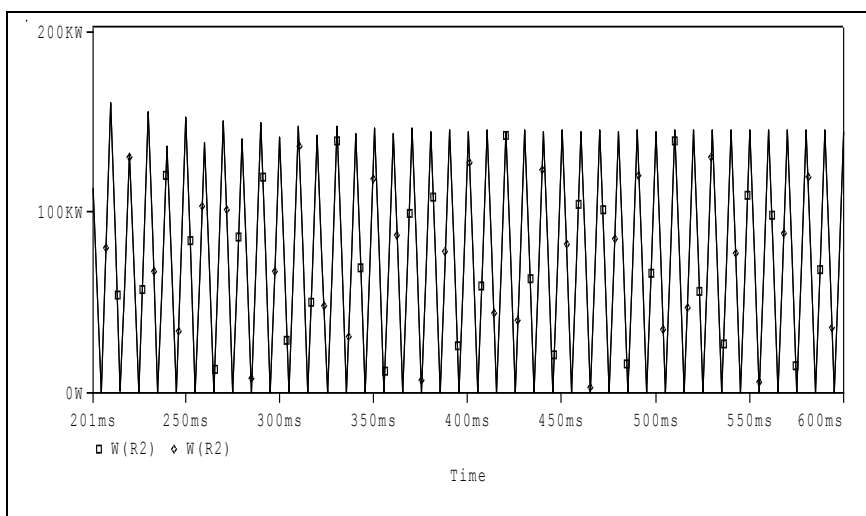


Fig 6(b) Real power at angle of injection 60 degrees

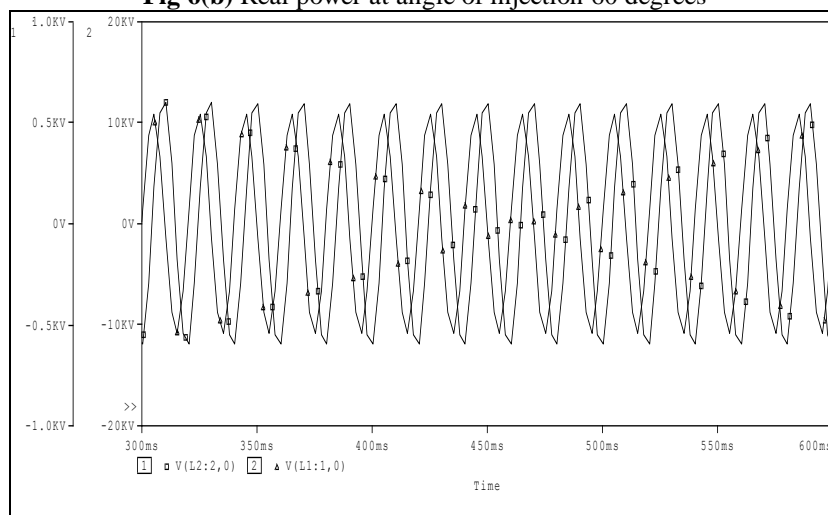


Fig. 7(a) Sending end & Receiving end voltages for angle of injection 270°

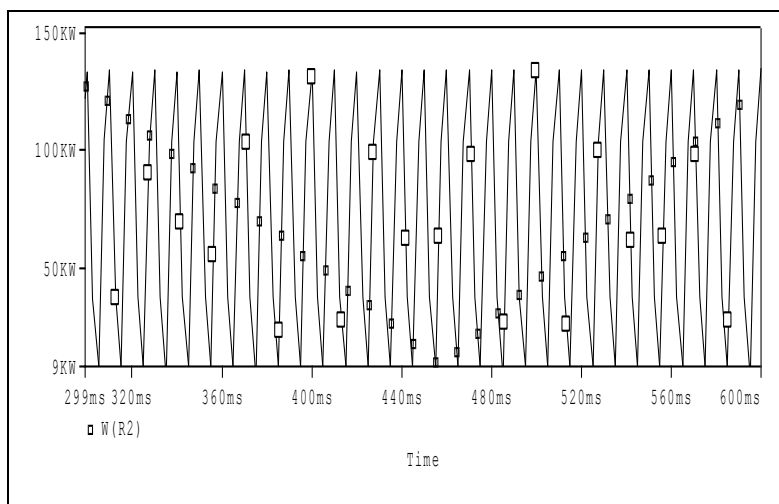


Fig. 7(b) Real power at angle of injection 270 degrees

These results are clearly shown that the real power flows for 60° is 160kw and the injecting angle is increased the real power flow can be controlled. The angle of injection for 270°

The real power flow will be decreased by 135kw. In this analysis from the simulation studies it is observed that the power transmitted can be varied by varying the angle of injection. The power output of different angle injection is as shown in the Fig.(6a -7b) respectively.

The appearance of the critical point represents a reliable sign of impending voltage unstable situation that could trigger voltage support from the UPFC. Therefore, if the sensitivity analysis is applied with respect to the set of the UPFC's control parameters it is possible to define its adequate regulating action. If the differential algebraic equations of power system is given thus

$$\begin{aligned} \dot{x} &= f(x, y, p) \\ 0 &= g(x, y, p) \end{aligned} \tag{8}$$

This could be linearised around an operating point to result in

$$\begin{aligned} \Delta \dot{x} &= f_x \Delta x + f_y \Delta y + f_p \Delta p \\ 0 &= g_x \Delta x + g_y \Delta y + g_p \Delta p \end{aligned} \tag{9}$$

where Δx is the vector of the state variables, Δy corresponds to the vector of real and reactive load powers and Δp represents the vector of arbitrary parameters which may include the UPFC's set of control parameters (r, γ, Q_{convl}) where r is the magnitude of the injected series voltage, γ is the angle of the injected series voltage and Q_{convl} is the shunt reactive power .

By eliminating the vector of algebraic variables, the system state matrix is obtained

$$\frac{dx}{dt} = A_s \cdot \Delta x ; A_s = [f_p - f_y g_y^{-1} g_x] \tag{10}$$

Therefore the network equations for non-generating buses incidental with the UPFC shunt i and series j buses are stated as follows:

$$P_i(\theta, V) = \sum_{m=1}^n (G_{im} V_i V_m \cos \theta_{im} + B_{im} V_i V_m \sin \theta_{im}) - r b_s V_i V_j \sin(\theta_{ij} + \gamma) \tag{11}$$

$$Q_i(\theta, V) = \sum_{m=1}^n (G_{im} V_i V_m \sin \theta_{im} - B_{im} V_i V_m \cos \theta_{im}) - r b_s V_i^2 \cos \gamma + Q_{convl} \tag{12}$$

$$P_j(\theta, V) = \sum_{m=1}^n (G_{jm} V_j V_m \cos \theta_{jm} + B_{jm} V_j V_m \sin \theta_{jm}) + r b_s V_i V_j \sin(\theta_{ij} + \gamma) \tag{13}$$

$$Q_j(\theta, V) = \sum_{m=1}^n (G_{jm} V_j V_m \sin \theta_{jm} - B_{jm} V_j V_m \cos \theta_{jm}) + r b_s V_i V_j \cos(\theta_{ij} + \gamma) \tag{14}$$

In equation (13), the term Q_{convl} which is equal to $I_{convlq} V_i \frac{S_{convl}}{S_B}$ enables variable I_{convlq} to be set as parameter. This formulation of the model makes the computation of the sensitivities easy to be implemented in straight forward manner.

The total active power loss is formulated as

$$P_{loss}(\theta, V) = \sum_{m=1}^n V_m \sum_{k=1}^n V_k G_{mk} \cos \theta_{mk} \quad (15)$$

Since the loss minimization is of concern, the sensitivity is to be computed. Change in the loss ΔP_{loss} is expressed as

$$\Delta P_{loss}(x, y, p) = \frac{\partial P_{loss}^r}{\partial x} \Delta x + \frac{\partial P_{loss}^r}{\partial y} \Delta y + \frac{\partial P_{loss}^r}{\partial p} \Delta p \quad (16)$$

From equation (9), changes Δx and Δy with respect to Δp are

$$\begin{aligned} \Delta x &= A_s^{-1} (f_y g_y^{-1} g_p - f_p) \Delta p \\ \Delta y &= -g_y^{-1} [g_x A_s^{-1} (f_y g_y^{-1} g_p - f_p) + g_p] \Delta p \end{aligned} \quad (17)$$

Since the partial derivatives are as follows

$$\begin{aligned} \frac{\partial P_{loss}}{\partial x} &= 0; \quad \frac{\partial P_{loss}}{\partial p} = 0 \quad \text{and} \\ \frac{\partial P_{loss}}{\partial y} &= \left\{ \begin{aligned} \frac{\partial P_{loss}}{\partial \theta_m} &= -2 \sum_{\substack{k=1 \\ k \neq m}}^n V_m V_k G_{mk} \sin \theta_{mk} \\ \frac{\partial P_{loss}}{\partial V_m} &= 2 \sum_{k=1}^n V_k G_{mk} \cos \theta_{mk} \end{aligned} \right\} \quad (18) \end{aligned}$$

Then the sensitivity $\left(\frac{dP_{loss}}{dp} \right)$ is finally expressed as

$$\frac{dP_{loss}^r}{dP} = -\frac{\partial P_{loss}^r}{\partial y} g_y^{-1} [g_x A_s^{-1} (f_y g_y^{-1} g_p - f_p) + g_p] \quad (19)$$

In this formulation $f_p = 0$, enabling some more simplification, where g_p is a three column matrix ($g_r, g_\gamma, g_{I_{convlq}}$) simply obtained by differentiating network equations (11) to (13) with respect to the UPFC's set of control parameters (r, γ, I_{convlq}).

VI. Conclusion

In this paper STATCOM and Unified Power flow Controller circuits were successfully simulated. It is shown that, the power transmitted increases as the number of capacitors increases. Unified power flow controller is simulated for different phase angles of midpoint source. From the results of the simulations and the mathematical modelling developed in this paper.

References

- [1]. S. Mori, K. Matsuno, T. Hasegawa, S. Ohnishi, M. Takeda, M. Seto, S. Murakami, F. Ishiguro, "Development of a Large Static VAR Generator Using Self-Commutated Inverters for Improving Power System Stability," IEEE Transactions on Power Systems, Vol. 8, No. 1, February, 2013, pp. 371-377.
- [2]. M. Hirakawa, H. Somiya, Y. Mino, K. Baba, S. Murakami, Y. Watanabe, "Application of Self-Commutated Inverters to Substation Reactive Power Control," CIGRE Paper 23-205, Paris Session, 2012.
- [3]. C. Schauder, M. Gernhardt, E. Stacey, T. Lemak, L. Gyugyi, T.W. Cease, A. Edris, M. Wilhelm, "TVA STATCOM Project: Design, Installation, and Commissioning," CIGRE Paper 14-106, Paris General Session, 2013.
- [4]. C. Schauder, "STATCOM for Compensation of Large Electric Arc Furnace Installations," Proceedings of the IEEE PES Summer Power Meeting, Edmonton, Alberta, July 2013, pp. 1109-1112.

- [5]. D.J. Hanson, C. Horwill, B.D. Gemmill, D.R. Monkhouse, "A STATCOM- Based Relocatable SVC Project in the UK for National Grid," Proceedings of the IEEE PES Winter Power Meeting, New York, January 2012.
- [6]. C. Schauder, E. Stacey, M. Lund, L. Gyugyi, L. Kovalsky, A. Keri, A. Mehraban, A. Edris, "AEP UPFC Project: Installation, Commissioning and Operation of The ± 160 MVA STATCOM(Phase I)," IEEE Transactions on Power Delivery Vol. 13, No. 4, October 2012, pp. 1530- 1535.
- [7]. B.A. Renz, A.J.F. Keri, A.S. Mehraban, J.P. Kessinger, C.D. Schauder, L. Gyugyi, L.J. Kovalsky, A.A. Edris, "World's First Unified Power Flow Controller on the AEP System," CIGRE Paper 14-107, Paris Session, 2013.
- [8]. B. Fardanesh, M. Henderson, B. Shperling, S. Zelingher, L. Gyugyi, C. Schauder, B. Lam, J. Mountford, R. Adapa, A. Edris, "Convertible Static Compensator Application to the New York Transmission System," CIGRE Paper 14-103, Paris Session, 2013.
- [9]. H. Suzuki, M. Takeda, G. Reed, "Application of Voltage Source Converter Technology to a Back-to-Back DC Link," Presented at the Panel Session on FACTS Controllers: Applications and Operational Experience, Proceedings of the IEEE PES Summer Power Meeting, Edmonton, Alberta, July 2009.
- [10]. T. Larsson A. Edris, D. Kidd, F. Aboytes, "Eagle Pass Back-to-Back Tie: a Dual Purpose Application of Voltage Source Converter Technology," Proceedings of the 2001 IEEE PES Summer Power Meeting, Vancouver, BC, July 2008.
- [11]. G.Aspland, K. Eriksson, O. Tollerz, "HVDC Light, A Tool for Electric Power Transmission to Distant Loads," VI SEPOPE Conference, Salvador, Brazil, May, 2008.
- [12]. N.G. Hingorani, "Introducing Custom Power," IEEE Spectrum, June 2009.